

# Direct load measurement of a Wind Turbine High Speed Shaft Bearing in the Field

Gary Nicholas, Tom Howard and Rob Dwyer-Joyce  
The Leonardo Centre for Tribology, The University of Sheffield  
Sheffield, South Yorkshire, S1 3JD, United Kingdom  
GNicholas1@sheffield.ac.uk

Jon Wheals, Dalil Benchebra  
Ricardo Innovations Ltd, Midlands Technical Centre  
Royal Leamington Spa, Leamington Spa, CV31 1FQ, United Kingdom  
Jonathan.Wheals@ricardo.com

## Abstract

Small piezoelectric transducers bonded to the outer raceway of a rolling element bearing can be used to send ultrasonic pulses to the element-raceway contact and receive reflections. Interpretation of the magnitude and time of flight (ToF) of the reflections can be used to deduce amount of load imparted between roller and raceway. The approach is most successful when the sensor is smaller than the area of contact. Then the sound field falls directly on the contact region. It is thus suited to *large* bearings, such as those found in wind turbines.

In this work, we have used the approach on the rotor side high speed shaft bearing in a Vestas V42 600 kW wind turbine operating in the Barnesmore windfarm in Northern Ireland. The bearing is a SKF 32222 tapered roller bearing. The nature of the contact geometry meant that careful location of the transducer was required to ensure direct pulse-echo reflection.

The load directly imparted by the roller onto the raceway can be deduced from the change in time of flight of the reflected signal. This measurement is challenging because the change in time of flight is only a few nanoseconds. Nevertheless loads on each roller were determined and results were consistent with expectation.

Functional over a period of 2 years, this validated method allows confident application in other sites such as pitch and main bearings to measure key inputs to prognostic algorithms derived from rig-based sensitivity studies, rather than optimistic ISO 281 calculations.

## 1. Introduction

Gearbox failures in wind turbines account for the longest downtime<sup>(1)</sup> and the most costly repairs<sup>(2)</sup>. Most of the failures within the gearbox are caused by bearing degradation<sup>(3)</sup>. Better understanding of bearing loading condition can be achieved through non-invasive direct ultrasonic monitoring. Information on bearing health can then be used to schedule maintenance and reduce unplanned downtimes.

Conventional wind turbines utilize Supervisory Control & Data Acquisition (SCADA) data to provide information on turbine operational, performance and maintenance condition. This data can then be used for failure prognostics and diagnostics<sup>(2)</sup>. More advanced condition monitoring systems utilize acoustic emissions, vibration, oil monitoring and ultrasonic techniques along with the SCADA data, mainly temperature measurements to predict and diagnose failure of wind turbine components<sup>(2)</sup>. However, acoustic emissions sensors are costly and due to its high sensitivity, signals are susceptible to noise which result in the requirement of extensive signal processing to yield meaningful data. Accelerometers are cheaper but inherit the same noise problem, which is more profound at low frequencies<sup>(4)</sup>. On the other hand, online oil monitoring systems are costly and periodic manual oil sample measurements are preferred instead<sup>(4)</sup>.

Active ultrasonic testing techniques are typically used in structural evaluation of wind turbine tower and blades and not in the gearbox<sup>(5,6)</sup>. Wave pulses are sent into the composite structures and the reflections or echoes received can be used to measure the thickness of different layers of laminate within the composite, and thus the potential to detect delamination<sup>(7)</sup>.

Ultrasonic measurements have previously been applied successfully within the laboratory environment on rolling element bearings for rolling bearing contact load measurements with good accuracy<sup>(8)</sup>. In this study, ultrasonic field measurements of a high speed shaft bearing obtained from a gearbox within a Vestas V42 wind turbine located in Barnesmore, Ireland were presented. This current study aims to demonstrate the capabilities of ultrasound to provide better understanding of real load cases within the bearing raceway-roller contact.

## 2. Background

The change in time of flight of pulses due to bearing loads can be used to determine the deflection of the raceway. The deflection can then be used to determine the bearing load through a simple elastic contact model.

The ToF change for a rolling bearing contact under loading is caused by three sources; surface deflection, acoustoelastic effect and phase shift<sup>(8)</sup>. Contribution from each source is important and thus cannot be neglected. By denoting the surface deflection as  $\delta$  and the speed of sound in the loaded raceway as  $(c_{zz})_p$ , the change in ToF due to deflection,  $\Delta t_\delta$  can be defined through equation (1).

$$\Delta t_\delta = \frac{2\delta}{(c_{zz})_p} \quad (1)$$

The acoustoelastic effect describes how the speed of the ultrasonic wave varies according to the state of stress of the medium it propagates through<sup>(8)</sup>. The ToF change due to the acoustoelastic effect alone,  $\Delta t_c$  is defined in equation (2) where  $L_{zz}$  is the acoustoelastic constant determined through experiment (for bearing steel  $L_{zz} = -2.24$ ) and  $(c_{zz})_0$  is the speed of sound in the unloaded raceway.

$$\Delta t_c = -\frac{2L_{zz}\delta}{(c_{zz})_0} \quad (2)$$

The apparent change in ToF due to phase change,  $\Delta t_\phi$  is given by equation (3) where  $\phi_R$  is the phase change between the unloaded signal and the reflected signal in loaded state and  $f$  is the centre frequency of the ultrasonic wave. The stiffness,  $K$  of the lubricant film is calculated by dividing the bulk modulus with the lubricant film thickness.

$$\Delta t_\phi = \frac{\phi_R}{2\pi f} \quad (3)$$

$$\phi_R = \arctan \frac{4\pi f K z_1 z_2^2}{K^2(z_1^2 - z_2^2) + (2\pi f z_1 z_2)^2} \quad (4)$$

By adding equations (1), (2) and (3), the total ToF change,  $\Delta t$  is given by equation (5). Through Hilbert Transform, the apparent change in ToF through phase shift can be eliminated. The roller contact load can then be obtained from the raceway deflection through Palmgren's empirical relationship<sup>(9)</sup> shown in equation (6) where  $P$  is the normal contact load in Newtons and  $l_0$  is the effective roller length in metres. Equation (7) can be formed by substituting equation (6) into (5) and eliminating  $\Delta t_\phi$ .

$$\Delta t = \frac{2(1-L_{zz})\delta}{(c_{zz})_0} + \frac{\phi_R}{2\pi f} \quad (5)$$

$$2\delta = 3.84 \times 10^{-8} \frac{P^{0.9}}{(l_0 \times 1000)^{0.8}} \quad (6)$$

$$P = \left[ \frac{\Delta t (c_{zz})_0 (l_0 \times 1000)^{0.8}}{(3.84 \times 10^{-8})(1-L_{zz})} \right]^{\frac{1}{0.9}} \quad (7)$$

### 3. Materials and methods

#### 3.1 Apparatus

Measurements were obtained from a high speed shaft inner raceway bearing located within the gearbox of an operational 600 kW Vestas V42 wind turbine located in Barnesmore, Ireland. The key specifications of the turbine are shown in Table 1. Figure 1 shows the instrumented bearing (marked as B) within the gearbox. The high speed shaft bearing is lubricated using VG320 gear oil.

**Table 1. Key specifications of the instrumented bearing**

Manufacturer	SKF
Type	32222 J2 tapered roller bearing
Rollers	20
Bore diameter	110 mm
Outer diameter	200 mm
Width	56 mm
Dynamic load rating	402 kN

Static load rating  
Fatigue load limit

570 kN  
61 kN

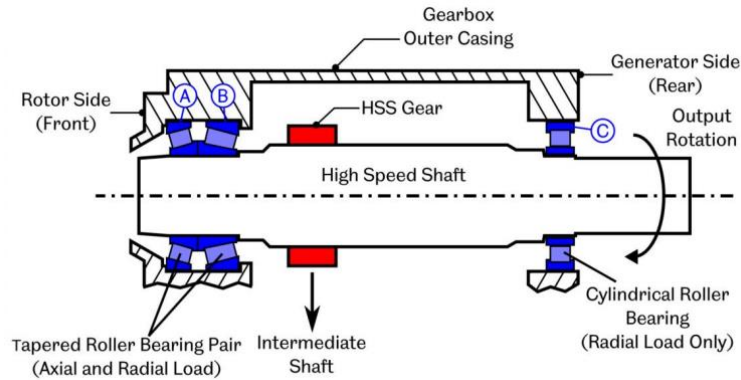


Figure 1. High speed shaft bearing configuration<sup>(10)</sup>

### 3.2 Ultrasonic instrumentation

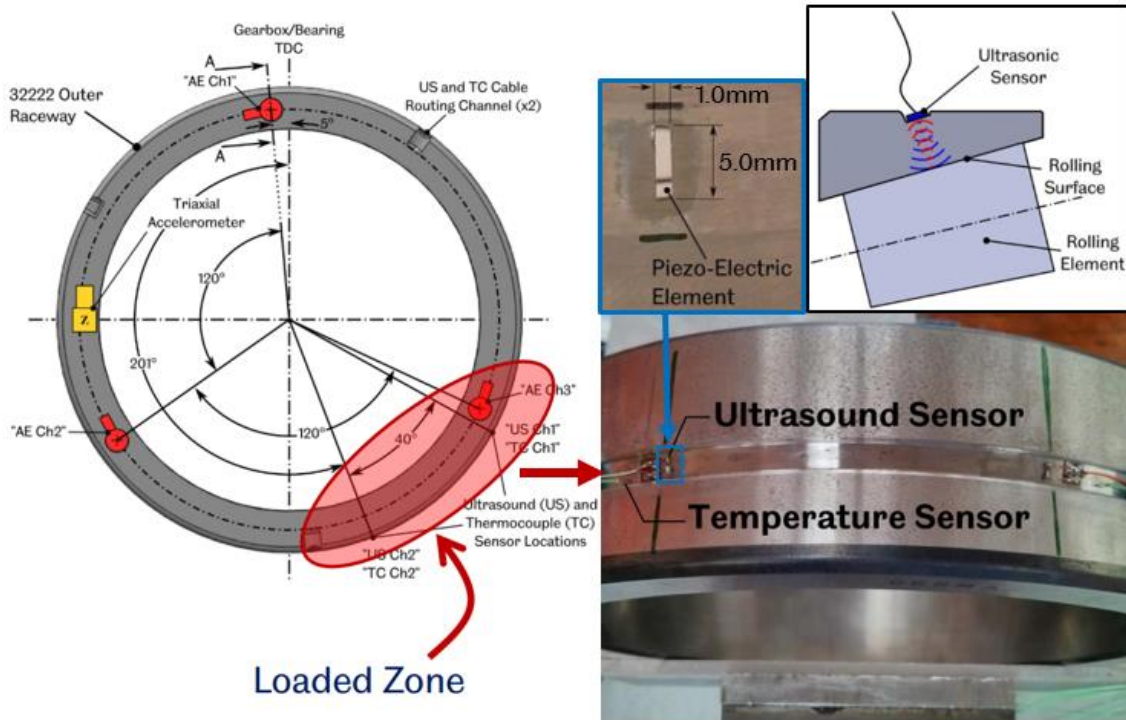


Figure 2. Sensors instrumented on the HSS bearing outer raceway<sup>(10)</sup>

To generate and receive ultrasonic pulses, piezo-electric elements were used, mounted onto the bearing outer race. The piezoelectric elements used had a thickness of  $0.2\text{ mm}$  corresponding to a central frequency of  $10\text{ MHz}$  and were cut to form rectangular strips of  $1\text{ mm} \times 5\text{ mm}$  to enhance their spatial resolution. Thermocouples were also installed adjacent to the ultrasonic elements to provide the closest approximation of the temperatures occurring at the contact under observation by each ultrasonic element. The positions of the two ultrasonic sensors with its thermocouple are shown in Figure 2.

Gearbox modelling results conducted by Ricardo were used to determine the position of the sensors. One sensor was positioned directly within the maximum loaded region whilst the other sensor was positioned on the edge of the maximum loaded region. The sensors operated in “pulse-echo” mode and the ultrasonic pulse receiver was used to excite the piezoelectric elements. The reflected signals were then digitized by the data acquisition system at 100 MHz and streamed into the computer for storage. Due to the high digitization rate, a time delay of 20 minutes was implemented between capture instances to avoid generating a large amount of data. During the capture window, one second of ultrasonic pulses were captured at a pulse repetition rate (PRR) of 80 kHz. The high PRR was necessary due to the high rotational speed of the bearing (1500 rpm) and subsequently the speed at which each rollers would move pass the ultrasonic elements. The sensors were bonded to the raceway surface using a high-temperature strain gauge adhesive having an upper operational temperature limit of 250 °C and wired with shielded coaxial cable. High temperature epoxy was used to seal the sensors against the lubricant.

#### 4. Results

Ultrasonic pulses with duration of 1  $\mu\text{s}$  were captured and compiled in real-time which forms the raw ultrasonic data streams shown in Figure 3 alongside its reference or unloaded pulse. The periodic reduction in signal amplitude within the data stream corresponds to the outer raceway-rolling element contact in which instance more energy is transmitted through. Five roller passes can be observed within the plots.

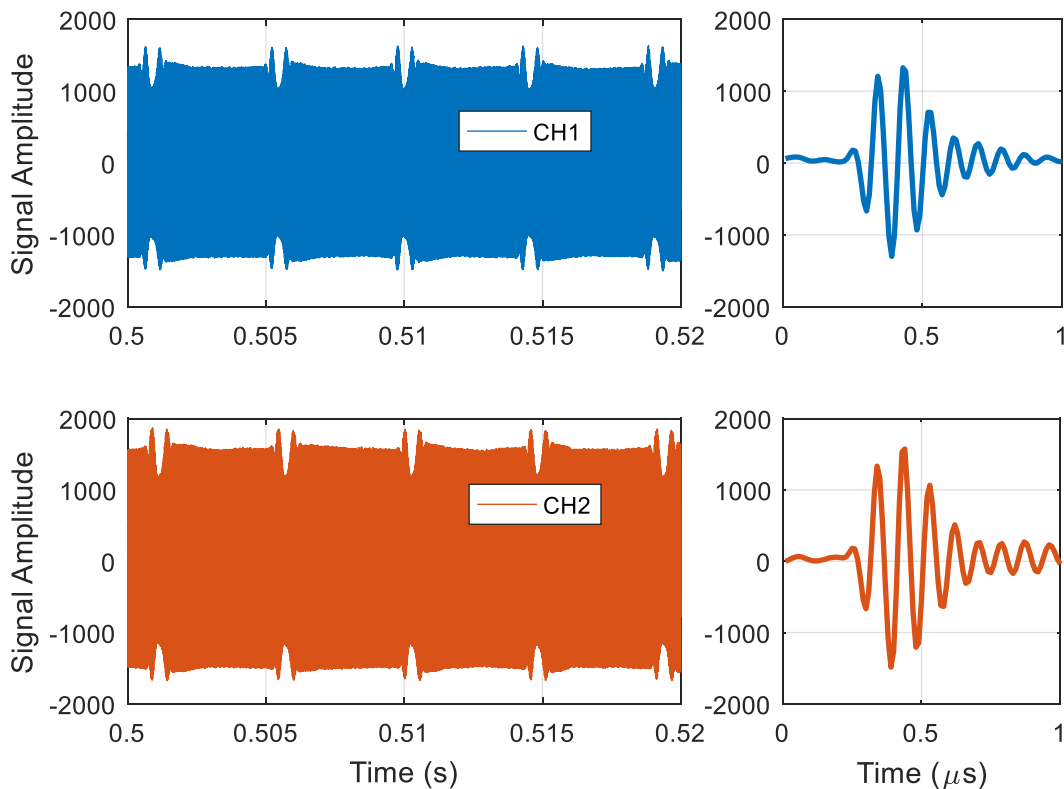


**Figure 3. Raw ultrasonic data from the two sensors**

Figure 4 shows the waveform of a loaded and unloaded pulse from Ch1, corresponding to a load of around 16 kN and their envelopes obtained through Hilbert Transform (HT).

Although the time shift is small (magnitude of nanoseconds), it can still be seen within the figure. The loaded pulse is seen to shift slightly towards left and this time shift is dependant on load.

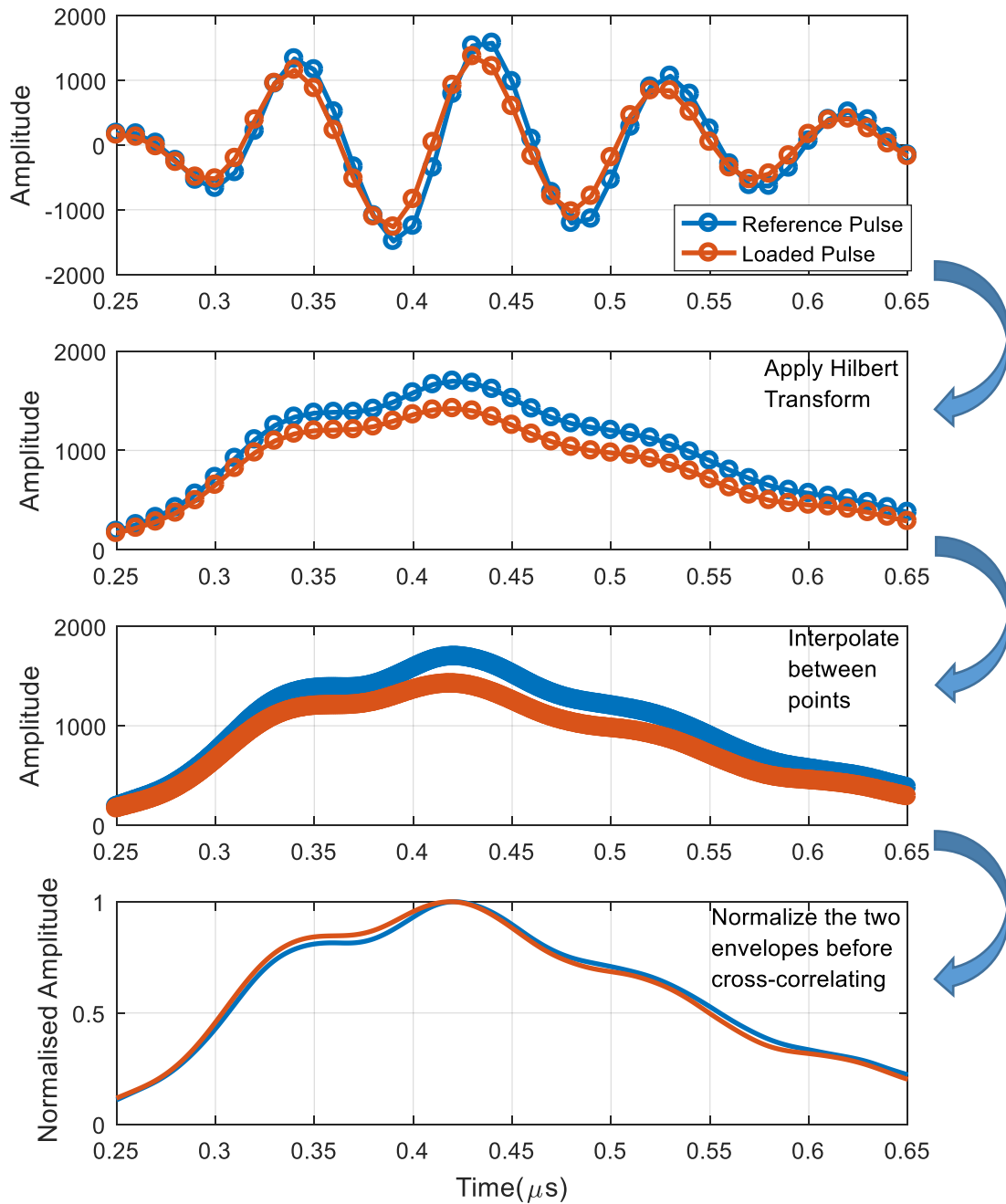


**Figure 4. Data processing carried out to obtain time shift**

As explained previously, to remove the effect of apparent time shift due to phase change, HT was carried which produces the pulse envelopes. As the time shift is computed to the closest sampling point, the accuracy of the method is limited to the ultrasonic pulse sampling frequency of 100 MHz. Thus, to improve accuracy, interpolation was performed on both reference and loaded envelopes to increase resolution before normalizing them

and performing cross correlation to obtain the time shift. The Palmgren equation (Equation 7) was then applied to obtain the load corresponding to them time shift.

Figure 5 shows the contact load measurements obtained after carrying out signal processing detailed previously. Two sets of data are shown from two sensors, individually positioned directly within and at the edge of the maximum loaded region. The peaks within the datasets correspond to the roller passing through the piezoelectric element. The datasets shown consist of 20 roller passes which corresponds to one bearing revolution.

It can be seen that the measured load on each roller varies, with the variation exhibiting a waviness across the rollers which is similar to the the change in time of flight observed across the rollers for a fixed load reported in previous work<sup>(8)</sup>. Load measurements on each roller ranges between 5 - 18 kN for sensor located at the edge of the maximum loaded region and 8 – 22 kN within the maximum loaded region. As expected, the average load measured from the sensor positioned at maximum loaded region is higher than the one positioned at the edge of the maximum loaded region.

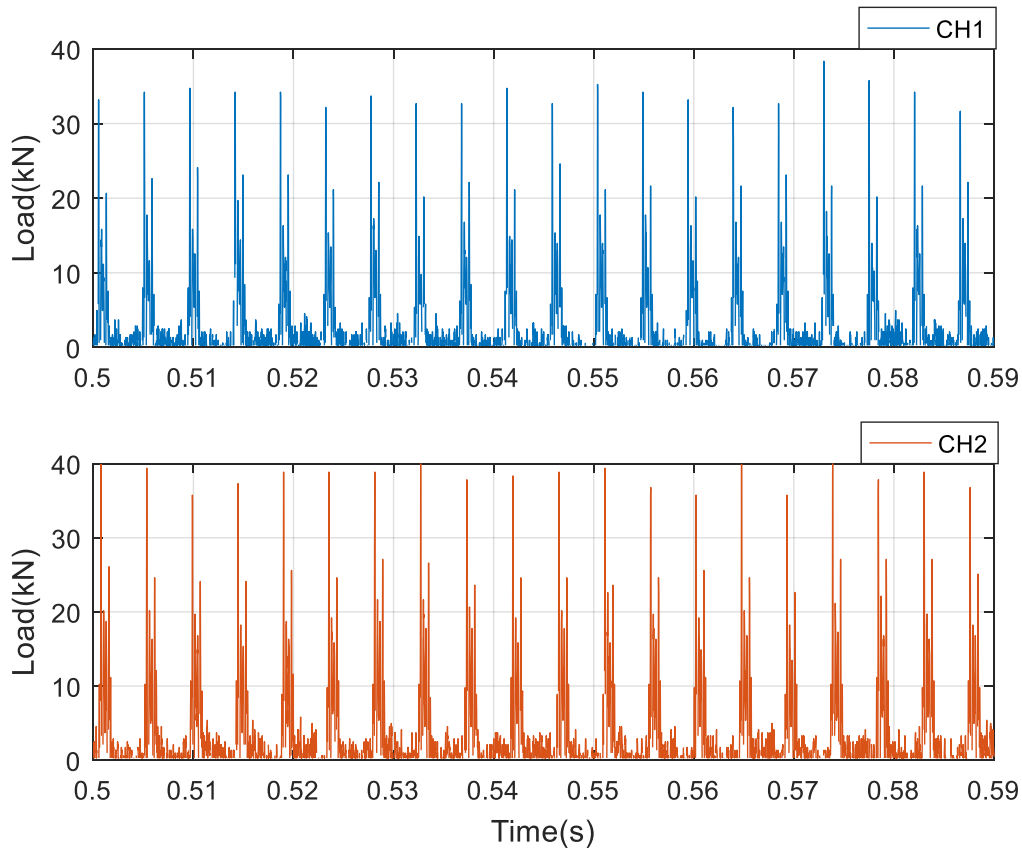


**Figure 5. Contact load measurements for both ultrasonic channels**

## 5. Conclusions

A method for on-line direct load measurement has been implemented on a field wind turbine gearbox bearing located in Ireland. Time shifts in the order of nanoseconds were

recorded and used to determine the roller-raceway contact load. Load measurements on each roller ranges between 5 - 18 *kN* for sensor located at the edge of the maximum loaded region (Ch1) and 8 – 22 *kN* within the maximum loaded region (Ch2). Variation of load across each rollers seem be periodic, which is similar to the the change in ToF observed across the rollers for a fixed load reported in previous work conducted.

## References

1. B Hahn, M Durstewitz, and K Rohrig, 'Reliability of Wind Turbines, Experiences of 15 Years with 1,500 WTs', Wind Energy, Berlin, 2007
2. K Kim, G Parthasarathy, O Uluyol, W Foslien, S Sheng, and P Fleming, 'Use of SCADA Data for Failure Detection in Wind Turbines, National Renewable Energy Laboratory (NREL), Golden, CO, USA, 2011
3. W Musial, S Butterfield, and B McNiff, 'Improving Wind Turbine Gearbox Reliability', European Wind Energy Conference, Milan, Italy, 2007
4. Z Hameed, Y S Hong, Y M Cho, S H Ahn and C K Song, 'Condition Monitoring and Fault Detection of Wind Turbines and Related Algorithms: A Review', Renewable and Sustainable Energy Reviews, pp 1-39, 2009
5. S K Chakrapani, V Dayal, R Krafka and A Eldal, 'Ultrasonic Testing of Adhesive Bonds of Thick Composites with Applications to Wind Turbine Blades', AIP Conference Proceedings 1430, 2012
6. S Li, K Shi, K Yang and J Xu, 'Research on the Defect Types Judgement in Wind Turbine Blades Using Ultrasonic NDT', Global Conference on Polymer and Composite Materials, 2015
7. P Tchakoua, R Wamkeue, T A Tameghe and G Ekemb, 'A Review of Concepts and Methods for Wind Turbines Condition Monitoring', Proceedings of the 2013 World Congress on Computer and Information Technology, Sousse, Tunisia, pp 1-9, June 2013
8. W Chen, R Mills and R Dwyer-Joyce, 'Direct Load Monitoring of Rolling Bearing Contacts using Ultrasonic Time of Flight', Proceedings of the Royal Society A, 2015
9. T A Harris, 'Rolling Bearing Analysis', 4<sup>th</sup> Edition, New York: John Wiley & Sons, 2001
10. T Howard, 'Development of a Novel Bearing Concept for Improved Wind Turbine Gearbox Reliability', PhD Thesis, Jan 2016